7116 *Inorg. Chem.* **2010**, *49*, 7116–7122
DOI: 10.1021/ic1009237

Inorganic Chemistry
Article

Oxalate Bridged Triangles Incorporating Mo_2^{4+} Units. Electronic Structure and Bonding

Malcolm H. Chisholm,*,† Nathan J. Patmore,*,‡ Carly R. Reed,† and Namrata Singh†

†*Department of Chemistry, The Ohio State University, 100 W. 18th Avenue, Columbus, Ohio 43210, and*
‡*Department of Chemistry, University of Sheffield, Sheffield S3 7HF, England*

Received May 9, 2010

The reactions between $[Mo_2L_2(CH_3CN)_6][BF_4]_2$ compounds and $[Bu^n_4N]_2[O_2CCO_2]$ in CH_3CN are shown to proceed under kinetic control to the formation of a mixture of molecular triangles and squares. The molecular triangles $[L_2Mo_2(O_2CCO_2)]_3$ **I** (L = DPhF, PhNCHNPh) and **II** (L = DAniF, *p*-MeO-C_6H_4NCHNC_6H_4-*p*-OMe) are the major products, and when 0.75 equivalents of $[Bu^n_4N]_2[O_2CCO_2]$ is employed, they are formed to the exclusion of the square. The molecular structure of **II** is reported based on a single crystal X-ray determination. The molecular triangles do not enter into an equilibrium with their molecular square counterparts in CH_2Cl_2, in contrast to their perfluoroterephthalate bridged counterparts. The compounds **I** and **II** are orange and have a strong electronic transition at $\lambda_{max} \sim 460$ nm assignable to metal-to-ligand charge transfer (^{1}MLCT) involving the oxalate bridge. Electronic structure calculations employing density functional theory on model compounds $[(HCO_2)_2Mo_2(O_2CCO_2)]_3$ and $[(HNCHNH)_2Mo_2(O_2CCO_2)]_3$ have been carried out and indicate the frontier occupied molecular orbitals are Mo_2 δ combinations e^4a^2, and the lowest unoccupied are bridge π^* for the formamidinates and δ^* for formates as ancillary ligands. Compounds **I** and **II** show quasi-reversible oxidation waves in their cyclic voltammograms and oxidation of **II** in 2-methyl-THF by reaction with $AgPF_6$ (1 equivalent) leads to a metal centered EPR signal, $g \sim 1.95$. The electronic absorption spectrum shows a low-energy broad band centered at 6418 cm^{-1}, which is assigned to an intervalence charge transfer (IVCT) band of a class III mixed valence ion.

Introduction

The design and synthesis of molecular assemblies have always been of interest to chemists, and the past two decades have seen significant advances.[1] Following the pioneering work of Fujita and Stang employing the use of square planar Pt(II) and Pd(II) units as corner pieces, Cotton and coworkers made extensive use of dinuclear M_2^{4+} units, where M = Mo and to a lesser extent Rh and Ru.[2−6] The paddlewheel motif of the Mo_2^{4+} quadruply bonded unit has a direct parallel with the square planar Pt(II) and Pd(II), and the most striking difference in the molecular assemblies arising from these two groups was that the former were neutral, while the latter (Pt(II) and Pd(II)) were charged. Also the Mo_2^{4+} units were redox active toward oxidation due to the facile $Mo_2^{4+/5+}$ couple which merely removes an electron from a δ orbital, whereas Pt(II) and Pd(II) do not readily form M(III) ions. Cotton's work established the existence of molecular loops, triangles, and squares of the type shown in Figure 1.

It was also shown that molecular loops and triangles and triangles and squares were sometimes present in a dynamic equilibrium.[8,9] For example, Cotton examined the equilibrium involving $[L_2Mo_2(O_2CC_6F_4CO_2)]_n$, where $n = 3$ and 4 and L = DAniF, and showed that the square, $n = 4$, was enthalpically favored but that entropy favored the triangle. This equilibrium could be monitored by variable temperature nuclear magnetic resonance (NMR) spectroscopy, and the thermodynamic enthalpies and entropies determined.[8]

Aside from rather preliminary electrochemical studies employing cyclic voltammetry, little is known about their electronic structure and the nature of the oxidized species.[7] In part, this was due to the presence of mixtures in solution.

Calculations in this laboratory on the oxalate bridged model compounds $[(HCO_2)_2M_2(O_2CCO_2)]_4$, where M = Mo

*To whom correspondence should be addressed. E-mail: chisholm@chemistry.ohio-state.edu.

(1) Northrop, B. H.; Yang, H.; Stang, P. J. *Chem. Commun.* **2008**, 5896–5908.
(2) Seidel, S. R.; Stang, P. J. *Acc. Chem. Res.* **2002**, *35*, 972–983.
(3) Cotton, F. A.; Lin, C.; Murillo, C. A. *Proc. Natl. Acad. Sci. U.S.A.* **2002**, *99*, 4810–4813.
(4) Angaridis, P.; Berry, J. F.; Cotton, F. A.; Murillo, C. A.; Wang, X. *J. Am. Chem. Soc.* **2003**, *125*, 10327–10334.
(5) Cotton, F. A.; Liu, C. Y.; Murillo, C. A.; Wang, X. *Inorg. Chem.* **2006**, *45*, 2619–2626.
(6) Fujita, M.; Yazaki, J.; Ogura, K. *J. Am. Chem. Soc.* **1990**, *112*, 5645–5647.
(7) Cotton, F. A.; Lin, C.; Murillo, C. A. *Acc. Chem. Res.* **2001**, *34*, 759–771.
(8) Cotton, F. A.; Murillo, C. A.; Yu, R. *J. Chem. Soc., Dalton Trans.* **2006**, *2006*, 3900–3905.
(9) Cotton, F. A.; Murillo, C. A.; Yu, R. *Inorg. Chim. Acta* **2006**, *359*, 4811–4820.

 Published on Web 07/01/2010

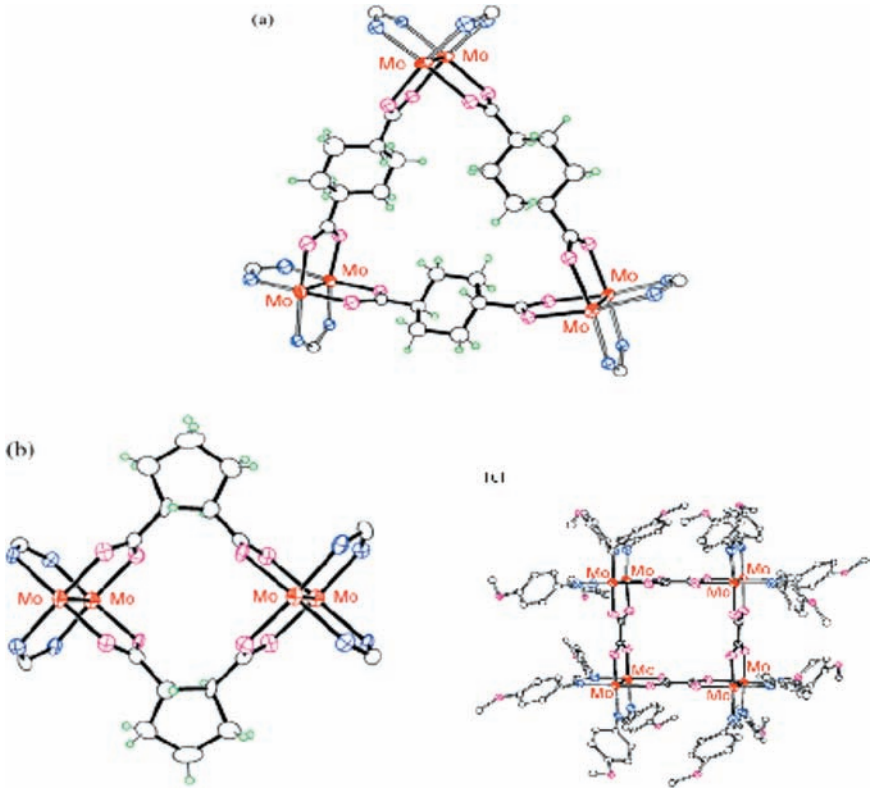

Figure 1. Representative examples of: (a) molecular triangle, (b) molecular loop, and (c) molecular square.[7]

or W, led us to believe that the singly oxidized molecular squares should be mixed valence cations of the fully delocalized kind, class III on the Robin and Day scheme.[10,11] Given the presence of the spin active nuclei ^{95}Mo and ^{97}Mo, having $I = 5/2$ with virtually identical magnetic moments and with combined natural abundance of ~25%, we believed that this matter could be easily established by electron paramagnetic resonance (EPR) spectroscopy, along with other spectroscopic techniques.

We report here our findings that were prompted by this line of reasoning which, as it turns out, pertain to the oxalate bridged molecular triangle containing Mo_2^{4+} corners rather than the square.

Experimental Section

General Information. All experiments, compound manipulations, and spectroscopic measurements were performed under an inert atmosphere using nitrogen-filled glove boxes and standard Schlenk line techniques. Solvents were distilled over the appropriate drying agent and stored over molecular sieves. Due to its instability, $[L_2Mo_2(O_2CCO_2)]_3^+$, where L = DAniF, was synthesized in situ by reaction of $[L_2Mo_2(O_2CCO_2)]_3$ with 1 equiv of $AgPF_6$ prior to spectroscopic measurements. $[Mo_2(DPhF)_2(CH_3CN)_6][BF_4]_2$ and $[Mo_2(DAniF)_2(CH_3CN)_6][BF_4]_2$ were prepared using published procedures.[12] The tetrabutylammonium salt of oxalic acid was prepared by neutralizing oxalic acid with 1.0 M Bu^n_4NOH in MeOH followed by vacuum drying at 55 °C for 18 h. The tetrabutylammonium salt of the ^{13}C oxalic acid was prepared similarly from $HO_2{}^{13}C{}^{13}CO_2H$ (Sigma Aldrich).

Electronic absorption spectra were recorded on a PerkinElmer Lambda 900 UV−vis/NIR spectrometer. ^{1}H NMR spectra were recorded on a 250 Bruker DPX Advance spectrometer and referenced to residual protio signals. Electrochemical measurements were performed using a Princeton Applied Research (PAR) 173A potentiostat−galvanostat equipped with a PAR 176 current-to-voltage converter using 0.1 M solutions of $Bu^n_4NPF_6$ in THF. The voltammetric cell was equipped with a platinum working electrode, a platinum wire auxiliary electrode, and a pseudoreference electrode consisting of a silver wire in 0.1 M $Bu^n_4NPF_6$/THF separated from the bulk solution by a Vycor tip. The potentials are referenced internally to the $FeCp_2^{0/+}$ couple by addition of a small amount of $FeCp_2$ to the solutions. X-band EPR spectra were recorded using a Bruker ESP300 electron spin resonance spectrometer. Temperature regulation was achieved by employing a Bruker variable temperature unit. Microanalysis was performed by Atlantic Microlab. Matrix-assisted laser desorption ionization time-of-flight (MALDI-TOF) mass spectra were obtained on a Bruker Microflex mass spectrometer provided by a grant from the Ohio BioProducts Innovation Center. The spectrometer was operated in a reflective, positive-ion mode. Laser power was used at the threshold level required to generate signal. Dithranol was used as the matrix and prepared as a saturated solution in THF.

Syntheses of Molecular Triangles. Synthesis of $[Mo_2(DPhF)_2(C_2O_4)]_3$, I. $[Mo_2(DPhF)_2(CH_3CN)_6][BF_4]_2$ (250 mg, 0.23 mmol) and $[Bu^n_4N]_2[O_2CCO_2]$ (132 mg, 0.23 mmol) were added to 200 mL of acetonitrile. The reaction mixture was stirred overnight. An orange solid was obtained by centrifugation and washed with 2 × 10 mL of acetonitrile. It was then dried under vacuum. Anal. calcd for $(Mo_2C_{30}H_{22}N_4O_8)_3$: C, 50.17; H, 3.31; N, 8.36%. Found: C, 49.12; H, 3.53; N, 8.19%. UV−vis (DMSO, 298 K,): 280, 430 nm. ^{1}H NMR (250 MHz; DMSO-d_6): δ 8.7 (1H, s); 7.1 (4H, m); δ 6.9 (6H, m). MALDI-TOF: Calculated monoisotopic MW for $C_{84}H_{66}Mo_6N_{12}O_{12}$: 2010.93. Found: 2010.2 (M^+). Calculated monoisotopic MW for $C_{112}H_{88}Mo_8N_{16}O_{16}$: 2681.91. Found: 2682.6 (M+).

(10) Bursten, B. E.; Chisholm, M. H.; D'Acchioli, J. S. *Inorg. Chem.* **2005**, *44*, 5571–5579.
(11) Robin, M. B.; Day, P. *Adv. Inorg. Radiochem.* **1967**, *10*, 247.
(12) Chisholm, M. H.; Cotton, F. A.; Daniels, L. M.; Folting, K.; Huffman, J. C.; Iyer, S. S.; Lin, C.; Macintosh, A. M.; Murillo, C. A. *J. Chem. Soc., Dalton Trans.* **1999**, 1387–1392.

Synthesis of $[Mo_2(DAniF)_2(C_2O_4)]_3$, II. The compound was prepared following a literature procedure.[13] UV−vis (DCM, 298 K,): 280, 470 nm. ^{1}H NMR (400 MHz; CH_2Cl_2-d_2): δ 8.69 (1H, s); 8.57 (0.74H, s); 6.65 (13H, m); 3.70 (9.5H, s). MALDI-TOF: Calculated monoisotopic MW for $C_{96}H_{90}Mo_6N_{12}O_{24}$: 2372.06. Found: 2370.5 (M^+). Calculated monoisotopic MW for $C_{128}H_{120}Mo_8N_{16}O_{32}$: 3163.08. Found: 3159.9 (M^+). Synthesis of the pure triangle $[Mo_2(DAniF)_2(C_2O_4)]_3$ without the square was obtained by modification of the published procedure involving less than 1 equiv of the oxalate salt. To a stirred solution of $[Mo_2(DaniF)_2(CH_3CN)_4][BF_4]$ (0.3476 g, 0.33 mmol) in 30 mL of CH_3CN was added $[Bu_4N]_2[C_2O_4]$ (0.1435 g, 0.25 mmol) in 30 mL of CH_3CN. A bright red precipitate formed immediately; the reaction was stirred overnight, washed with 2 × 20 mL CH_3CN, and dried under vacuum. The crude product was extracted with CH_2Cl_2 and layered with hexanes for recrystallization. ^{1}H NMR (400 MHz; CH_2Cl_2-d_2): δ 8.70 (1H, s); 6.65 (8H, dd); 3.70 (6H, s). MALDI-TOF: 2369.7 (M^+). Crystals suitable for X-ray diffraction were grown by dissolving **II** in 1,2-Cl_2-C_6H_4 and layering with hexane.

In the case where a solution of $[Mo_2(DAniF)_2(CH_3CN)_4][BF_4]$ (0.0917 g, 0.088 mmol) in 30 mL of CH_3CN was added to a stirring solution of $[Bu_4N]_2[C_2O_4]$ (0.0539 g, 0.094 mmol) in 10 mL of CH_3CN, both species were observed in the precipitate that formed with the triangle being the dominant species. ^{1}H NMR (400 MHz; CH_2Cl_2-d_2): δ 8.69 (1H, s); 8.57 (0.85 H, s); 6.65 (16H, m); 3.70 (11H, s).

Electronic Structure Calculations. The geometries of the model compounds $[Mo_2(O_2CH)_2]_3(\mu$-$C_2O_4)_3$ and $[Mo_2(H_2N_2CH)_2]_3(\mu$-$C_2O_4)_3$ were optimized in the gas-phase using density functional theory with the aid of the Gaussian03 suite of programs. The B3LYP functional was used along with the Stuttgart−Dresden (SDD) energy consistent pseudopotentials for molybdenum and the 6-31G* basis set for all remaining atoms. Optimizations were performed in D_{3h} symmetry for the $[Mo_2(O_2CH)_2]_3(\mu$-$C_2O_4)_3$ model compound and C_{3h} symmetry for $[Mo_2(H_2N_2CH)_2]_3(\mu$-$C_2O_4)_3$ and confirmed to be minima on the potential energy surface using harmonic vibrational frequency analysis. All Gauss View plots are shown at an isosurface value 0.02.

X-ray Crystallography. X-ray crystallographic data for complex **II** were collected on a Bruker Smart CCD area detector with an Oxford Cryosystems low-temperature system. After integration of the raw data and merging of equivalent reflections, an empirical absorption correction was applied (SADABS) based on comparison of multiple symmetry-equivalent measurements.[14] The structures were solved by direct methods and refined by full-matrix least-squares on weighted F^2 values for all reflections using the SHELX suite of programs.[15] All hydrogens were included in the model at calculated positions in both structures using a riding model with $U(H) = 1.5 \times U_{eq}$ (bonded carbon atom) for methyl hydrogens and $U(H) = 1.2 \times U_{eq}$ (bonded carbon atom) for aromatic hydrogens.

Two of the 1,2-dichlorobenzene solvent molecules were located and modeled with isotropic displacement parameters. The structure contains voids (888 Å^3) comprised of a further five disordered 1,2-dichlorobenzene solvent molecules that could not be effectively modeled. By symmetry, there are four such regions in the unit cell. The data were subjected to the SQUEEZE subroutine of PLATON,[16] to remove this contribution of electron density from the intensity data. The experimental data relating to structural determination is shown in Table 1.

Table 1. Crystallographic Data for **II**·7(1,2-Cl_2-C_6H_4)

empirical formula	$C_{138}H_{108}Cl_{14}Mo_6N_{12}O_{24}$
FW	3390.30
T (K)	100(2)
λ (Å)	0.71073
crystal system	monoclinic
space group	$P2_1/c$
a (Å)	16.7412(6)
b (Å)	25.6515(9)
c (Å)	32.0808(12)
α (deg)	90
β (deg)	103.617(2)
γ (deg)	90
V (Å^3)	13 389.4(8)
Z	4
d_{calc} (Mg m^{-3})	1.682
μ (mm^{-1})	0.901
F_{000}	6808
θ range (deg)	1.03−25.00
index ranges	$-19 \le h \le 19$ $-30 \le k \le 30$ $-37 \le l \le 38$
reflections collected	143 133
independent reflections	23 563 [R(int) = 0.0633]
observed reflections [$I > 2\sigma(I)$]	14603
data completeness to θ_{max}	1.000
data/restraints/parameters	23 563/72/1283
goodness-of-fit on F^2 [a]	1.046 [1.492]
final R indices [$I > 2\sigma(I)$][a]	R_1 = 0.0748 [0.1356], wR_2 = 0.2164 [0.3944]
R indices (all data)[a]	R_1 = 0.1187 [0.2353], wR_2 = 0.2368 [0.4640]
largest diff. peak and hole (e Å^{-3})[a]	1.661/−1.363 [5.258/−1.391]

[a] Statistics prior to the treatment of data with the SQUEEZE subroutine of PLATON are bracketed.

Results and Discussion

Syntheses. The preparation of the molecular triangles involved the reaction between the salts $[Mo_2L_2(CH_3CN)_6][BF_4]_2$ and $[Bu^n_4N]_2[O_2CCO_2]$ in acetonitrile at room temperature leading to **I** (L = PhNCHNPh, DPhF) and **II** (L = p-OMe-C_6H_4NCHNC_6H_4-p-OMe, DAniF). In these reactions the neutral products were precipitated as formed. The precipitates also contained some of the molecular square as a minor product. The relative ratio of the triangles to the square was readily determined by ^{1}H NMR spectroscopy upon integration of the formamidinate methine resonance that appears near 8.5 ppm. See Figure 2.

The molecular square $[Mo_2(DAniF)_2(O_2CCO_2)]_4$ was originally reported along with the formation of six other molecular Mo_2^{4+} containing assemblies of which three others were crystallographically characterized as squares.[13] The crystallographically characterized molecular squares had the following bridges: oxalate, fumarate, 1,1′-ferrocenedicarboxylate, and 4,4′-biphenyldicarboxylate. In this original report Cotton stated that while the four compounds have been shown to be square in the crystalline state there is no guarantee that a transformation to triangles in solution does not occur. Cotton further stated, "For each of the seven compounds, the ^{1}H NMR spectrum showed one signal for the methine protons, one for the CH_3 groups, and only a single mulitplet for the aromatic hydrogen atoms. This implies a highly symmetric structure, such as a triangle or a square, but does not tell us which. It cannot even be used to rule out a mixture in solution, as shown by the case of the $[Rh_2(DAniF)_2(O_2CCO_2)]_{3/4}$ mixture, where there was no doubling of the ^{1}H signals despite the presence of both species in comparable amounts."

As we show quite clearly here, in our synthesis of $[Mo_2(DAniF)_2(C_2O_4)]_n$, following the orginial procedure, two

(13) Cotton, F. A.; Lin, C.; Murillo, C. A. *Inorg. Chem.* **2001**, *40*, 478–484.
(14) Sheldrick, G. *SADABS*; University of Göttingen, Göttingen, Germany, 1996.
(15) *SHELXTL*, version 5.1;Bruker Analytical X-ray Instruments Inc.: Madison, WI, 1998.
(16) Spek, A. L. *J. Appl. Crystallogr.* **2003**, *36*, 7–13.

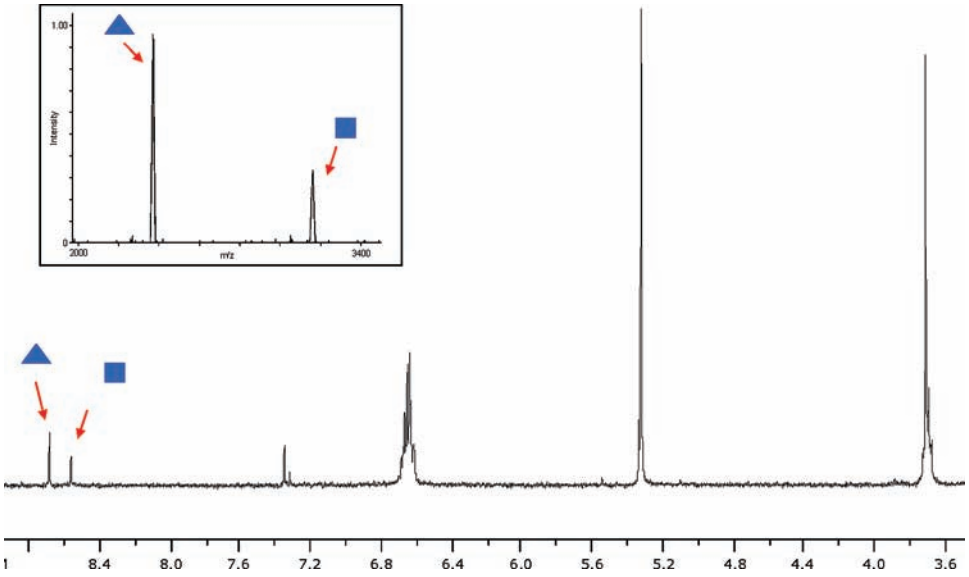

Figure 2. ^{1}H NMR for compound **II** in CD_2Cl_2 and MALDI-TOF for compound **II** (inset) showing the presence of the molecular square.

compounds are formed and each gives rise to distinct methine ^{1}H resonances (the minor one of which corresponds to that assigned to the square by Cotton) and two distinct molecular ions. We can only surmise that in the original work the single crystals selected for the X-ray study were also employed in the ^{1}H NMR study. We have also seen that recrystallization of this mixture from a 1,2-dichlorobenzene and diethyl ether layer led to the isolation of crystals of the triangle suitable for X-ray analysis as shown in Figure 3.

We were naturally curious about the possible equilibrium involving a square and a triangle for the oxalate bridged complexes and examined the temperature dependence of the ^{1}H signals, since this technique had been successfully applied for examination of the equilibrium of the perfluoroterephthalate bridged triangles and squares.[8] In the case of **II**, the relative ratio of the triangle and square was invariant with temperature which led us to believe that the two were formed under kinetic control (see Supporting Information). As a test of this we examined the reactions involving $[Mo_2(DAniF)_2(CH_3CN)_6][BF_4]_2$ and varying ratios of $[Bu^n{}_4N]_2[O_2CCO_2]$, namely 0.25, 0.5, and 0.75. In each case the precipitated product from the reaction in CH_3CN was examined by MALDI-TOF; all showed the formation of **II** in the absence of the square (see Supporting Information).

Moreover, in solution the presence of **II** can be seen by ^{1}H NMR in the absence of the signal assigned to the square (Figure 4). We feel that these results conform to the view that for this oxalate bridged compound there is not a kinetically labile equilibrium between the square and the triangles.

In our studies, we have found it very difficult to isolate the triangle **I** *completely* free from its square counterpart when both compounds are formed under conditions described originally by Cotton and co-workers. Both compounds are orange and moderately air sensitive. Compound **II** is appreciably soluble in CH_2Cl_2 and $CHCl_3$, while **I** is only very sparingly soluble in these solvents but appreciably soluble in DMSO. However, in reactions involving 0.75−0.80 equiv of $[Bu^n{}_4N]_2[O_2CCO_2]$,

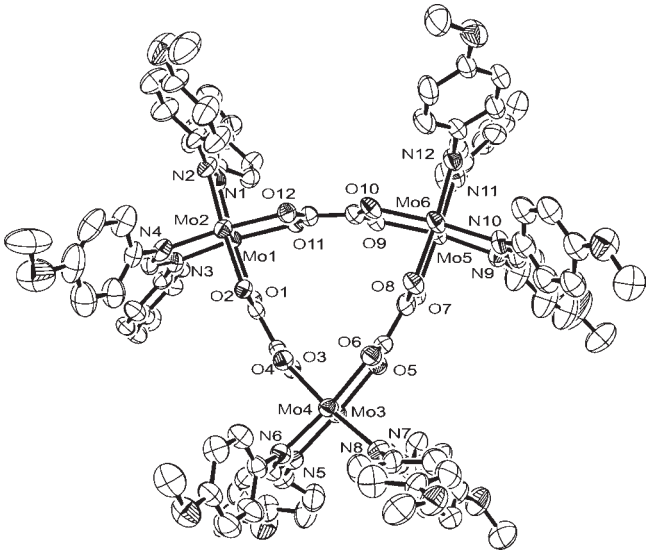

Figure 3. Molecular structure of complex **II**·7(1,2-Cl_2−C_6H_4), with anisotropic displacement parameters drawn at the 50% level. Hydrogen atoms and solvent molecules are omitted for clarity. Selected bond distances and angles are given in the Supporting Information.

the triangles are formed in preference to the mixture, and recrystallization allows their isolation in pure form. In an attempt to prepare the molecular square in preference to the triangle, we have carried out an inverse addition wherein the $[Mo_2]^{2+}$ cation was added to ∼1.1 equiv of $[Bu^n{}_4N]_2[O_2CCO_2]$ in CH_3CN. However, this resulted in a similar 4:3 ratio of the triangle to square as determined by ^{1}H NMR from the formamidinate methine signal.

Electronic Structure Calculations. In our earlier computational studies, we considered the bonding in the model compounds $[(HCO_2)_2M_2(O_2CCO_2)]_4$, where M = Mo or W, and found that the M_2 δ orbitals split in the ascending order of energy a_{1g}, e_u, and b_{2g} in the symmetry point group D_{4h}.[10] The a_{1g} orbital is the totally symmetric combination of the M_2 δ's that mix with the oxalate π^* and are thus stabilized by back bonding. Thus, upon oxidation to generate the cationic species $[(HCO_2)_2M_2(O_2CCO_2)]_4^+$,

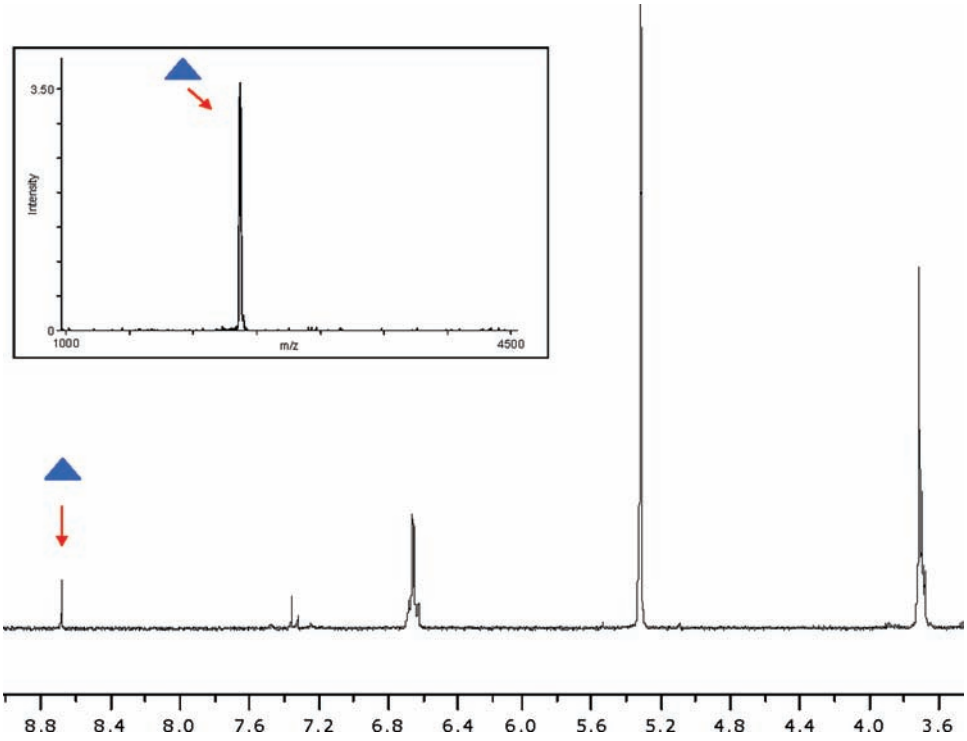

Figure 4. ^{1}H NMR in CD_2Cl_2 and MALDI-TOF of product of reaction between 1.0 equiv of $[Mo_2(DaniF)_2(CH_3CN)_4][BF_4]$ and 0.75 equiv of $[Bu_4N]_2[C_2O_4]$.

we would anticipate the frontier molecular orbital configuration to be $a_{1g}{}^2e_u{}^4b_{2g}{}^1$. Furthermore, based on the knowledge that the cations $[(Bu^tCO_2)_3MM]_2(\mu\text{-}O_2CCO_2)^+$, where MM = Mo_2, MoW, and W_2, are fully delocalized, class III mixed valence (MV) ions on the Robin and Day scheme, we anticipated that the molecular square MV ion would be similarly fully delocalized.[17]

In order to investigate the electronic structure of the oxalate bridged triangles, we carried out electronic structure calculations employing density functional theory (DFT) as implemented by Gaussian03 on the model compounds $[(HCO_2)_2Mo_2(O_2CCO_2)]_3$ and $[(HNCHNH)_2Mo_2(O_2CCO_2)]_3$ in D_{3h} and C_{3h} symmetry, respectively.

The frontier molecular orbital energy diagram shown in Figure 5 compares the formate and formamidinate triangles.

In both cases the highest energy occupied orbitals (HOMO) are the e and a combinations of the M_2 δs, and of these, the a orbital is stabilized by back bonding to the oxalate bridge. These orbitals are shown in Figures 6 and 7 as Gauss View plots.

The HOMO is the doubly degenerate e orbital (HOMO in Figures 6 and 7), and the calculated energy separation between the e and a Mo δ combinations is a measure of the degree of electronic coupling of the Mo_2 centers. The magnitude of the energy splitting is similar for the formate 0.53 eV and the formamidinate 0.43 eV. These values may be compared to the calculated splitting of the M_2 δ combinations in the squares, which are larger, and in the dimer of dimers, M = Mo, 0.40 and 0.30 eV for the formate and formamidinate complexes, respectively. To some extent the Mo_2 δ to oxalate π interactions are weakened in the molecular triangle relative to the square because the angles are not optimum for overlap. Nevertheless the Gauss View plots of the a orbital reveal a significant Mo_2 δ−oxalate π* mixing, and the calculations imply a greater splitting of the δ combinations in the triangle relative to the dimer of dimers. Also in comparing formates and formamidinates, we note that the splitting of the δ orbital combinations is greater for the formates. This is a consequence of the greater Mo to N π bonding that effectively reduces the back bonding to the oxalate. Alternatively stated, the M_2 δ orbitals mix more strongly with the formamidinate N 2p orbitals relative to the formate oxygen 2p orbitals, and this in turn lessens the M_2 δ oxalate π bonding in the formamidinates. The lowest energy vacant orbitals are a and e combinations

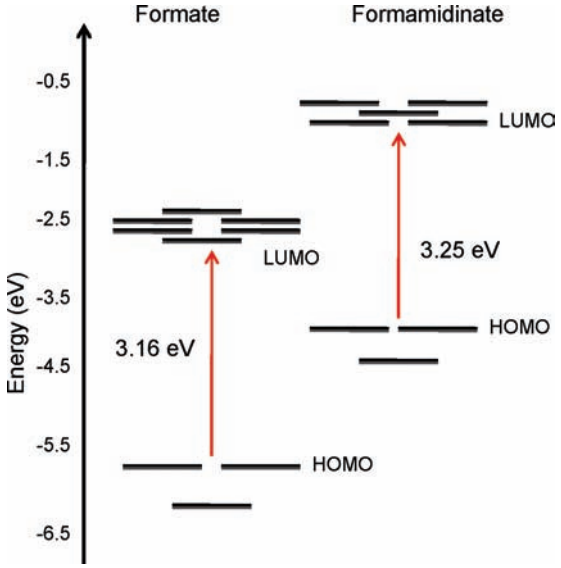

Figure 5. Frontier molecular orbital energy diagram comparing the $[Mo_2]_3$[formate]$_3$ and $[Mo_2]_3$[formamidinate]$_3$ triangles.

(17) Chisholm, M. H.; Patmore, N. J. *Can. J. Chem.* **2009**, *87*, 88–94.

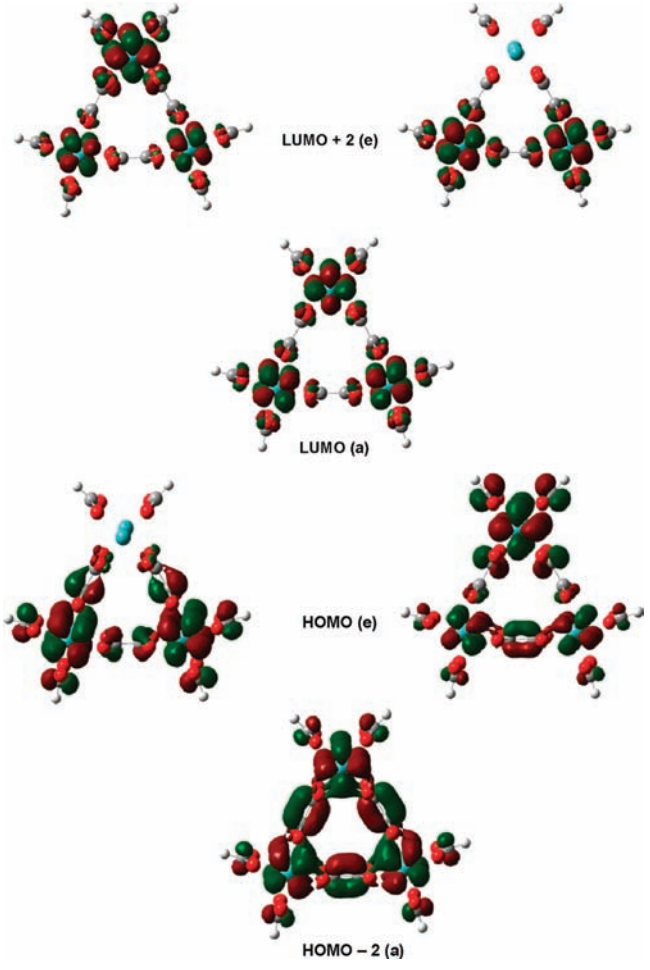

Figure 6. Frontier molecular orbitals for the model compound $[Mo_2(O_2CH)_2]_3(\mu\text{-}C_2O_4)_3$.

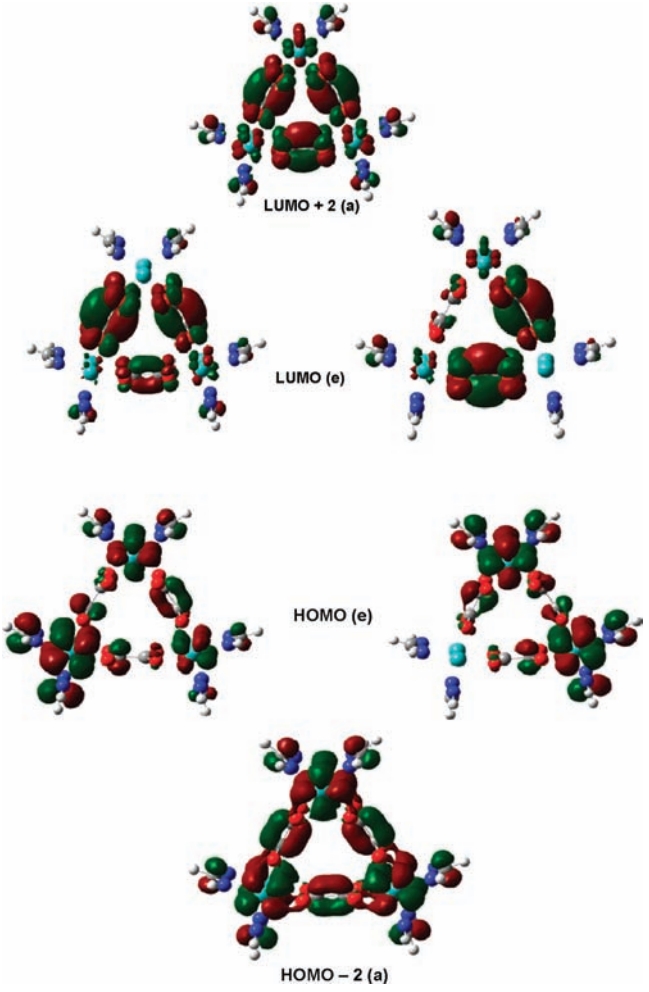

Figure 7. Frontier molecular orbitals for the model compound $[Mo_2(H_2N_2CH)_2]_3(\mu\text{-}C_2O_4)_3$.

of oxalate π^* (mixing with M_2 δ) and the M_2 δ^* orbitals. In the case of the formate triangle, the Mo_2 δ^* a and e combination lies just below that of the oxalate π^*, but for the formamidinate this situation is reversed. However, for both molecular triangles we anticipate fully allowed electronic transitions involving the M_2 δ and bridge π^*, ^{1}MLCT at a similar energy. See Figure 5.

One final note is that the frontier orbital energies of the formamidinate triangle lies >1 eV higher in energy relative to the formate. This is a consequence of the greater electron-donating ability of the formamidinate, and experimentally this is seen in the electrochemical oxidation potentials of M_2 δ orbitals as a function of formamidinates versus carboxylates in their respective homoleptic compounds.

For example, the first oxidation potentials of $[(Bu^tCO_2)_3Mo_2]_2(O_2CCO_2)$ and $[(DAniF)_3Mo_2]_2(O_2CCO_2)$ are -0.03 and -0.18 V with respect to the $Cp_2Fe^{0/+}$ couple.[18,19]

Electronic Absorption Spectra. The electronic absorption spectra for the two compounds **I** and **II** are shown in Figure 8. The intense ($\varepsilon \sim 19\,600$ $M^{-1}cm^{-1}$) absorption in the visible region of the spectrum at λ_{max} 460−470 nm accounts for the orange color of the compounds, and this is readily assignable to metal-to-bridge charge transfer as anticipated by the calculation on the model compound.

Treatment of a CH_2Cl_2 solution of **II** with 1 equiv of $AgPF_6$ yielded a silver metal precipitate, and the electronic absorption spectrum of $\mathbf{II}^+$ revealed a relatively weak and broad band in the near IR centered around 1500 nm.

Plotted in energy units this absorption is $\sim$6418 cm^{-1}, and we estimate a half width of $\sim$2885 cm^{-1} (Figure 9). This may be compared with the low-energy absorption for the cation $[L_3Mo_2]_2(O_2CCO_2)^+$, where L = ^{t}BuCO$_2$, that is centered around 3200 cm^{-1} and has a non-Gaussian envelope typical of compounds of class III MV ions that are close to the II/III border.[20] We therefore conclude that the singly oxidized radical cation is behaving as a delocalized ion. If we assume the Hush equation for the half width of IVCT bands, namely $\Delta\nu_{1/2} = (2310\ \nu_{max})^{1/2}$ can be applied to $\mathbf{II}^+$, then the calculated half width is predicted to be 3850 cm^{-1}, which is certainly larger than our experimental estimate.[21] Assuming a class III ion, the value of H_{ab} is $\sim$3200 cm^{-1}, roughly twice that observed for the dimer of dimers.[18] Consistent with the greater calculated orbital separation between the M_2 δ combinations in the triangle, we also note that some broadening of this IVCT or charge resonance band may be expected because of Jahn−Teller effects for the molecular orbital

(18) Chisholm, M. H.; Patmore, N. J. *Acc. Chem. Res.* **2007**, *40*, 19–27.
(19) Cotton, F. A.; Donahue, J. P.; Lin, C.; Murillo, C. A. *Inorg. Chem.* **2001**, *40*, 1234–1244.
(20) Chisholm, M. H.; Pate, B. D.; Wilson, P. J.; Zaleski, J. M. *Chem. Commun.* **2002**, *2002*, 1084–1085.
(21) Hush, N. S. *Prog. Inorg. Chem.* **1967**, 391.

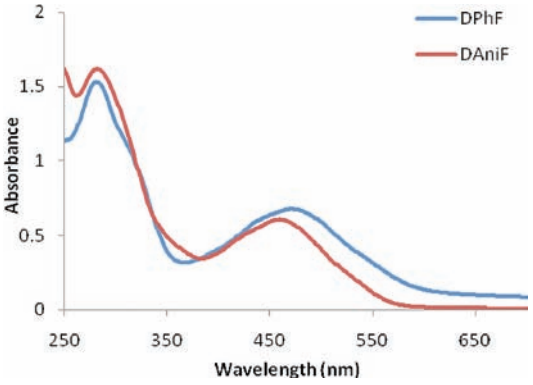

Figure 8. Electronic absorption spectra for compounds **I** and **II**, recorded in THF at ambient temperature.

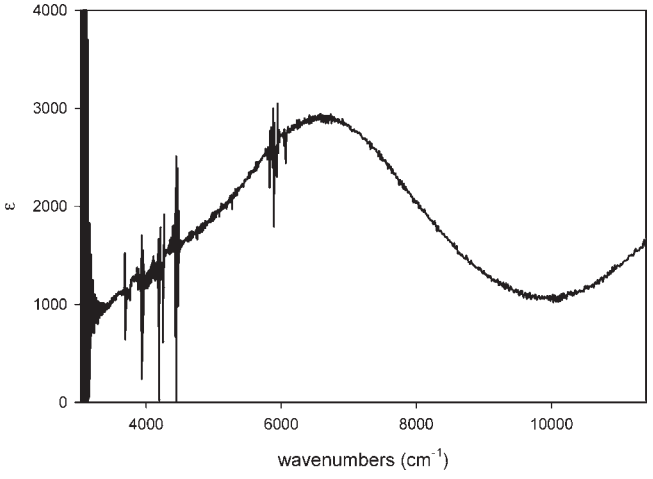

Figure 9. Electronic absorption spectra for compound $\mathbf{II}^+$ in CH_2Cl_2.

configuration a^2e^3. Finally, we note that comparisons of H_{ab} involving the theories of mixed valence ions that traditionally involve two redox centers are not necessarily valid for three, as in $\mathbf{II}^+$, and as such the ion $\mathbf{II}^+$ is simply better described as delocalized.

Electrochemical Studies. Both compounds show a reversible oxidation wave corresponding to the formation of $\mathbf{I}^+$ and $\mathbf{II}^+$ at −160 and −330 mV, respectively, with the $FeCp_2^{+/0}$ couple set 0.0 V. Compound **I** was studied in DMSO and showed a second quasi-reversible oxidation wave at 58 mV. Compound **II** was studied in THF and showed two further oxidation waves at −180 and −3 mV, neither of which were fully reversible. Complex II was also studied in CH_2Cl_2 with similar results. The triangle **II** thus shows similar oxidation characteristics to its isomeric molecular square, as reported by Cotton et al., though the absolute oxidation potentials for the three successive oxidations cannot reasonably be compared given the differences in electrochemical set ups and solvents (see Supporting Information, Figures S3 and S4).[13]

EPR Spectrum of Radical Cation $\mathbf{II}^+$. To a sample of **II** dissolved in 2-methyl THF was added less than 1 equiv of $AgPF_6$, and the EPR spectrum of the resultant solution was recorded in the range from 150 to 293 K. The spectrum of the liquid solution at 222 K is shown in Figure 10.

At no temperature were we able to resolve a satellite spectrum due to the presence of the spin-active nuclei $^{95/97}Mo$, $I = 5/2$. This may have been due to the presence of the ^{14}N nuclei, $I = 1$, bonded to Mo, and we note that unlike the EPR spectrum of $Mo_2(O_2CBu^t)_4^+$, the spectrum of $Mo_2(DAniF)_4^+$ similarly shows no resolved hyperfine satellites in our hands.[22] Another potentially line-broadening effect could arise from the fact that in a delocalized situation the molecular orbital configuration a^2e^3 would be subject to a Jahn−Teller distortion. We can only conclude that the EPR signal at g = 1.95 confirms the metal-based nature of the oxidation. This *g* value is similar to the 1.94 value reported for the cations $[(Bu^tCO_2)_3Mo_2]_2(O_2CCO_2)^+$ and $Mo_2(O_2CBu^t)_4^+$, which show hyperfine coupling to $^{95/97}Mo$ of 14 and 27 Hz, respectively.[18,22] Regrettably the absence of any hyperfine coupling in the spectrum of $\mathbf{II}^+$ does not allow us to comment on the degree of delocalization of the unpaired electron on the EPR time scale.

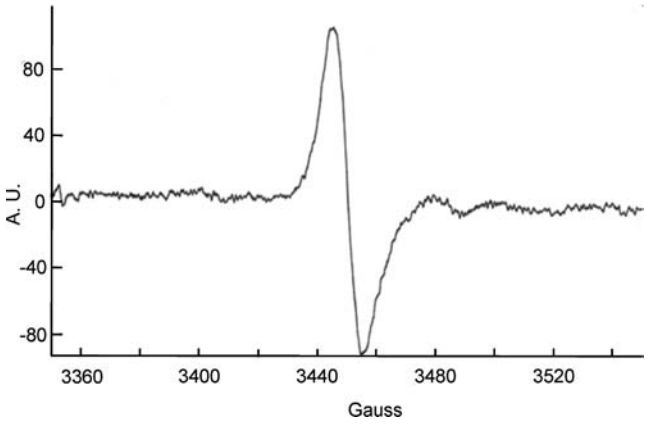

Figure 10. EPR spectrum of $\mathbf{II}^+$ at 222 K in 2-methyl THF.

Conclusions

The present study has revealed that the molecular triangles **I** and **II** are not in equilibrium in solution with their respective molecular squares but rather that the triangle and the square are formed in competition, with the triangle being kinetically favored. Electronic structure calculations imply a significant degree of Mo_2 δ-oxalate bridge π* bonding with a separation of the a and e Mo_2 δ combinations being ~0.5 eV. The preliminary evidence presented here suggests that the radical cation $\mathbf{II}^+$ is a fully delocalized class III ion, though EPR spectroscopy did not confirm this because of the lack of a resolved hyperfine spectrum. Further studies are, however, planned to probe the detailed nature of the oxidized species, $\mathbf{II}^+$, and the dynamics of charge distribution of these triangles in their MLCT photoexcited states.

Acknowledgment. We thank the Ohio Supercomputer Center for providing computational time and resources, Dr. G. Renkes for help with the EPR experiment, and Mr. Harry Adams for crystallographic assistance. N.J.P. gratefully acknowledges the Royal Society for the award of a University Research Fellowship.

Supporting Information Available: Selected bond distances and angles are given. Reaction results involving $[Mo_2(DAniF)_2(CH_3CN)_6][BF_4]_2$ and varying ratios of $[Bu^n{}_4N]_2[O_2CCO_2]$, namely 0.25, 0.5, and 0.75; precipitated product from the reaction in CH_3CN was examined by MALDI-TOF. This material is available free of charge via the Internet at http://pubs.acs.org.

(22) Chisholm, M. H.; D'Acchioli, J. S.; Pate, B. D.; Patmore, N. J.; Dalal, N. S.; Zipse, D. J. *Inorg. Chem.* **2005**, *44*, 1061–1067.